

## $d_{5/2}$ isobaric analog state in $^{57}\text{Co}$ from $^{56}\text{Fe}(p,\gamma)$ and $^{56}\text{Fe}(p,p'\gamma)$ reactions

S. El-Kateb\* and M. Garwan†

*Department of Physics, University of Petroleum and Minerals, Dhahran 31261, Saudi Arabia*

(Received 3 April 1986)

The resonances at  $E_p=3774$  and  $3794$  keV in  $^{57}\text{Co}$  are identified as fragments of the  $d_{5/2}$  isobaric analog resonance from  $^{56}\text{Fe}(p,\gamma)$  and  $^{56}\text{Fe}(p,p'\gamma)$  reactions. Gamma-decay schemes and angular distributions have been studied. From angular distributions and symmetry potential considerations, the level at  $4675$  keV in  $^{57}\text{Co}$  is considered to be the antianalog state. The  $M1$  transition strength of the analog-antianalog state has been measured and is compared with theoretical predictions. Additional information on the  $M1$  strength systematics in the isovectorial  $\frac{5}{2}^+ \rightarrow \frac{5}{2}^+$  transitions in the  $f$ - $p$  shell nuclei is provided.

### I. INTRODUCTION

The behavior of  $M1$  gamma-ray transitions from isobaric analog states (IAS's) with  $J=l+\frac{1}{2}$  to antianalog states (AIAS's) in  $1f$ - $2p$  shell nuclei has frequently been investigated in the past both from an experimental and a theoretical viewpoint (see Ref. 1 and references therein). As these IAS's are of parallel spin alignment, one anticipates enhancement in the  $M1$  strengths for IAS→AIAS, unlike the reduction seen for those of antiparallel spin alignment ( $J=l-\frac{1}{2}$ ). However, for the  $p_{3/2}$  IAS in these nuclei,  $M1$  strengths are found to be hindered by a factor of 100 compared to the single-particle (s.p.) estimates. Such hindrance has been qualitatively understood as a consequence of mixing core excitations into the wave function describing the antianalog final state for the radiative transition, thereby reducing their s.p. character.

Exceptions to the hindered  $M1$  strengths in the  $1f$ - $2p$  shell odd  $A$  nuclei are the IAS→AIAS transitions having parent states of positive parity such as  $\frac{5}{2}^+$  and  $\frac{9}{2}^+$ , since these states are expected to have large s.p. strengths. Furthermore, the number of configurations with which these states ( $\frac{5}{2}^+$  or  $\frac{9}{2}^+$ ) may mix for  $A \leq 65$  is severely reduced since the other states in this mass region have negative parity. Thus it may be expected that these positive parity states are of simpler structure than their neighboring negative parity states. However, available data from  $(p,\gamma)$  resonant reactions<sup>1,2</sup> for  $\frac{9}{2}^+$  states (e.g., Co, Cu, Ga, and As isotopes) showed wide variations in the  $M1$  strengths from one nucleus to another through the  $f$ - $p$  shell. Attempts to interpret such reduction have been made by several authors.<sup>3-5</sup> They resort to the interference induced by various kinds of core excitation acting within the lower isospin components.

In the case of  $d_{5/2}$  states, IAS→AIAS  $M1$  strengths have been studied for few medium odd  $A$  nuclei. For  $^{59}\text{Cu}$  the  $M1$  strength<sup>6</sup> is about 14% of the s.p. estimate. At the upper end of the  $1f$ - $2p$  shell the  $M1$  strength<sup>2,7</sup> value is reduced to 1% in  $^{65}\text{Ga}$  and  $\sim 0.4\%$  in  $^{73}\text{As}$ . However, the strength of this transition<sup>2</sup> starts to increase again in  $^{75}\text{As}$  to 5% of the s.p. estimate. To understand better the systematics of the associated  $M1$  strengths be-

tween IAS→AIAS for  $d_{5/2}$  states, further data on target nuclei whose  $1f_{7/2}$  proton shell is not completely filled would be very useful.

Several research groups<sup>8-10</sup> have surveyed the energy range where the  $d_{5/2}$  IAS's are expected using  $(p,p)$ ,  $(p,p_0)$ ,  $(p,p')$  and  $(p,p'\gamma)$  reactions on  $^{56}\text{Fe}$  targets. However, the reported results still show some disagreements. A further investigation is necessary in order to resolve some of the discrepancies reported earlier. With this in mind, we studied the  $^{56}\text{Fe}(p,\gamma)$  and  $^{56}\text{Fe}(p,p'\gamma)$  reactions to locate the  $d_{5/2}$  IAS in  $^{57}\text{Co}$  which corresponds to the 2506 keV state in the parent nucleus  $^{57}\text{Fe}$ , and investigated the IAS→AIAS strength.

In this paper we describe in detail the results of the investigations of the  $d_{5/2}$  isobaric analog resonances (IAR) in  $^{57}\text{Co}$ . The preliminary results of part of this work have been published elsewhere.<sup>1</sup> Emphasis is laid here on locating the IAR and AIAS, and determining the spin assignment of both IAS's and AIAS's as well as the  $M1$  strengths between IAS→AIAS for  $d_{5/2}$  IAR in  $^{57}\text{Co}$ .

### II. EXPERIMENTAL PROCEDURE AND ANALYSIS

A proton beam from the 5.5 MV tandem Van de Graaff accelerator at the nuclear research center "Demokritos" in Greece was used to bombard isotopically enriched (99.93%)  $^{56}\text{Fe}$  targets which were 1–6 keV thick for 3 MeV protons. The targets were prepared by vacuum evaporation of the isotopic material in the form of  $\text{Fe}_2\text{O}_3$  onto  $20 \mu\text{g}/\text{cm}^2$  thick carbon or 0.13 mm thick tantalum backing. These targets were directly cooled with a mixture of methanol and distilled water during the experiment and showed no apparent deterioration under the beam currents of approximately 1–7  $\mu\text{A}$  which were used. A small tantalum lined target chamber of 2 cm radius was used. A  $20 \mu\text{g}/\text{cm}^2$  thick  $^{56}\text{Fe}$  target on carbon backing was used for measuring the excitation curves and singles  $\gamma$ -ray spectra, while a  $60 \mu\text{g}/\text{cm}^2$  thick  $^{56}\text{Fe}$  target on tantalum backing was used for the angular distribution measurements. A negative bias of 300 V was applied to the target chamber to suppress secondary electron emission. Calibration of the beam energy was carried out us-

ing the resonance at  $E_p = 1746.6 \pm 0.9$  keV in the  $^{13}\text{C}(p,\gamma)^{13}\text{N}$  reaction.<sup>11</sup> The uncertainty in the energy calibration was found to be within 1 keV of the energy inferred from the nuclear magnetic resonance (NMR) value of the analyzing magnet. The overall resolution of the system, including the beam spread, but excluding target thickness effect, was about 750 eV.

A 48 cm<sup>3</sup> cylindrical coaxial Ge(Li) detector having a resolution of 1.87 keV full width at a half maximum (FWHM) for 1.33 MeV  $\gamma$  rays was used to detect the  $\gamma$  rays for the excitation function, singles  $\gamma$  spectra, and angular distribution measurements. The efficiency function of the 48 cm<sup>3</sup> Ge(Li) detector for  $\gamma$  rays of energies of up to 11 MeV in the geometry of the experiment was determined by measuring the  $\gamma$ -ray yields from the resonance at  $E_p = 1.381$  MeV in the  $^{27}\text{Al}(p,\gamma)^{28}\text{Si}$  reaction, as well as calibrated radioactive sources. The branching ratios for the  $\gamma$  rays in the  $^{27}\text{Al}(p,\gamma)^{28}\text{Si}$  reaction were taken from Ref. 12.

The gamma-ray excitation function was measured in steps of approximately 1.5 keV each with the Ge(Li) detector at 90° with respect to the proton beam direction and 3 cm distance from the target center. Gates were set on the multichannel analyzer to detect the 845 keV ( $2^+ \rightarrow \text{g.s.}$ ) transition in  $^{56}\text{Fe}$ , and  $\gamma$  rays with energies between 4 and 5 MeV, 7 and 10 MeV, and 8.7 and 10 MeV. Each point on the excitation function was obtained for a charge of 200  $\mu\text{C}$  of the integrated beam. After locating the resonances, singles  $\gamma$ -ray spectra for an integrated charge of 14 mC were taken on and off resonance.

For angular distribution measurements, the 48 cm<sup>3</sup> Ge(Li) detector was placed 7 cm from the target and spectra were recorded at four angles with  $\theta = 0^\circ, 30^\circ, 60^\circ,$  and  $90^\circ$ . In each measurement a charge of 10–16 mC was collected. Another 45 cm<sup>3</sup> Ge(Li) detector with a measured resolution of 2 keV FWHM at 1.33 MeV was used as a monitor at  $\theta = -90^\circ$ . Off-resonance measurements were also made for the same charge as for the resonance run in order to correct for background and possible interference from nearby resonances. Two independent normalizations were available, in addition to the integrated charges; the intense 845 keV  $2^+ \rightarrow \text{g.s.}$  transition in  $^{56}\text{Fe}$  and sometimes intense (p, $\gamma$ ) lines from the monitor allowed compensation for small beam energy changes during long angular distribution measurements. The eccentricity of the measuring geometry was checked, using as reference the isotropic angular distribution of the 844 keV ( $2^+$ )  $\gamma$  ray from the  $^{27}\text{Al}(p,p'\gamma)$  reaction. The eccentricity correction was found to be less than 1%.

All  $\gamma$ -ray spectra were analyzed by conventional means to obtain  $\gamma$ -ray energies and intensities. The  $\gamma$ -ray energy calibration was achieved by the use of a  $^{60}\text{Co}$  source and the contaminant  $\gamma$  rays<sup>13</sup> from the  $^{19}\text{F}(p,\alpha\gamma)^{16}\text{O}$  reaction at  $6129.41 \pm 0.18$  keV and the  $^{18}\text{O}(p,\alpha\gamma)^{15}\text{N}$  reaction at  $5269.6 \pm 0.3$  keV. In forming the decay scheme for each resonant state, attention was paid both to proper energy sums and intensity balance. The branching percentages presented are thought to have an absolute precision of  $\pm 3\%$  or better.

The measured intensities at the four angles were least squares fitted to determine the coefficients in the Legendre

polynomial expansion,

$$W(\theta_i) = \sum_{k=0}^{k_{\max}} A_k P_k(\cos\theta_i).$$

The coefficients  $A_k$  normalized to unit intensity by division by  $A_0$  were then corrected for the detector solid angle attenuation coefficients  $Q_k$ . Further analysis to obtain possible spin values for resonances and bound states and to determine the  $\gamma$ -ray multipole mixing ratio  $\delta$  was carried out using a chi-squared ( $\chi^2$ ) test. In the analysis of the angular distribution data a computer program based on the factored formalism of Harris, Hennecke, and Watson<sup>14</sup> was used. The phases of the multipolarity mixing ratios used in the formalism are the same as those used by Ferguson.<sup>15</sup> In this program the general correlation function is

$$W(\theta_1, \theta_2, \phi) = \sum_{KMN} A_{KM}^N Q_K Q_M X_{KM}^N(\theta_1, \theta_2, \phi),$$

which is given in terms of population parameters defining the relative populations of the magnetic substates of the state being populated in the reaction. For unpolarized protons bombarding a spin-zero target nucleus, as in the present study, only one parameter (the multipole mixing ratio  $\delta$ ) enters the least squares fit of the experimental data to the theoretical correlation function. Using the  $\chi^2$  test, possible spin values were tested by calculating the quantity

$$Q^2 = \frac{1}{N} \sum_i \Delta\omega_i [W(\theta_i) - W^*(\theta_i)]^2.$$

In this case  $N$  is the number of degrees of freedom,  $\Delta\omega_i$  is the statistical weight factor,  $W(\theta_i)$  is the experimental intensity measured at the  $i$ th of a set of detector angles  $\theta_i$ , and  $W^*(\theta_i)$  is the theoretical intensity at  $\theta_i$ , which is a function of the assumed spins and multipole mixing ratios.

For each possible spin assignment the value of  $Q^2$  was calculated in steps of  $2^\circ$  in  $x$ , where  $x = \tan^{-1}\delta$ . In the case where there is a statistically significant agreement between the experimental data and the theoretical values calculated from the correlation function, the minimum  $Q^2$  value is near unity. Hence acceptable spin values  $J$  and  $\delta$  are those for which  $Q^2$  can be made approximately equal to unity. Spins were rejected if  $Q^2$  did not fall below the value corresponding to the 0.1% confidence level for any value of  $x$ . The estimates of errors associated with the mixing ratio  $\delta$  were obtained at  $Q^2 = Q_{\min}^2$ , corresponding to one standard deviation for  $Q_{\min}^2$ .

### III. RESULTS

#### A. Excitation function and decay schemes

The gamma ray yield from the  $^{56}\text{Fe}(p,\gamma)$  and  $^{56}\text{Fe}(p,p'\gamma)$  reactions was measured in the energy range  $E_p = 3760$ – $3840$  keV using a target of approximately 1 keV thickness on carbon backing. The result of these measurements is shown in Fig. 1. This energy region is of particular interest in the present work, since evidence for the

analog of the  $d_{5/2}$  state at 2506 keV in the parent nucleus  $^{57}\text{Fe}$  is anticipated.

We have investigated the decays of the strongest resonances in this energy region, namely at  $E_p=3774$  and  $3794$  keV. Both resonances showed an intense  $\gamma$ -ray transition to the ground state (g.s.) of  $^{57}\text{Co}$ . Furthermore, both resonances populated a state at 4675 keV as well as other low spin states with significant strength. Figure 2 shows the high energy portion of the  $\gamma$ -ray spectra measured at the 3774 and 3794 keV resonances, together with a spectrum taken at an off-resonance energy ( $E_p=3786$  keV) for comparison with the on-resonance spectra. The

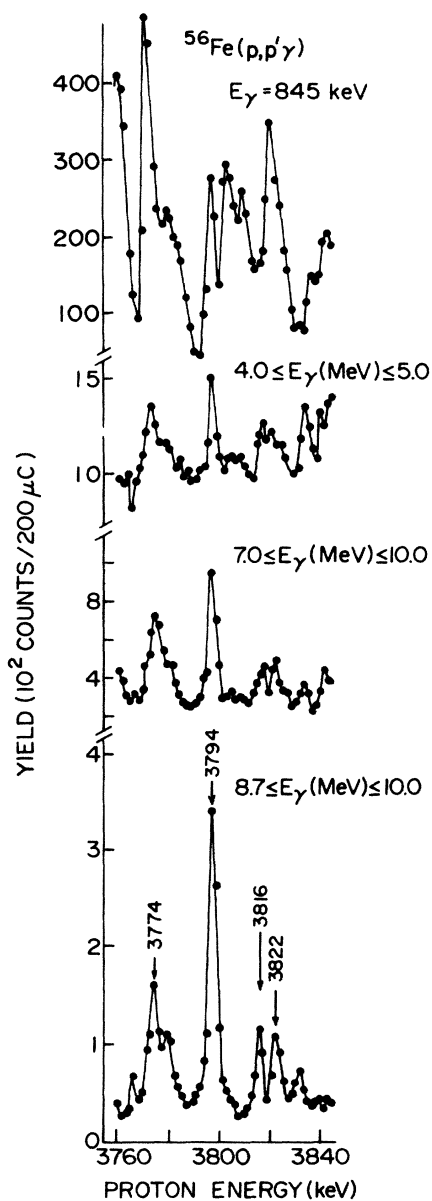


FIG. 1. Excitation functions for the  $^{56}\text{Fe}(p,p'\gamma)$  and  $^{56}\text{Fe}(p,\gamma)^{57}\text{Co}$  reactions in the incident proton energy range  $E_p=3760$ – $3840$  keV.

decay scheme for both resonances, including the branching ratios of the primary transitions, is shown in Fig. 3. The indicated energies and  $J^\pi$  values for the resonance levels and the level at 4675 keV are from the present work and are in good agreement with our preliminary results.<sup>1</sup> The other two resonances at  $E_p=3816$  and  $3822$  keV are relatively weaker and showed the contaminant  $\gamma$  rays at 5270 and 6130 keV (see Fig. 1). Both resonances were found to populate the  $\frac{7}{2}$  g.s. as well as other low spin states in  $^{57}\text{Co}$  with no significant strength.

## B. Angular distributions and spin assignments

Gamma-ray angular distributions were measured for the strong resonances at  $E_p=3774$  and  $3794$  keV. Table I summarizes the normalized Legendre polynomial coefficients and their associated uncertainties for the transitions studied at each resonance. Figures 4 and 5 show the least squares fits to the experimental data. The analyses of the  $\gamma$ -ray angular distributions from the  $^{56}\text{Fe}(p,\gamma)$  and  $^{56}\text{Fe}(p,p'\gamma)$  reactions at the two resonances will be discussed individually.

### 1. Angular distribution of $\gamma$ rays from the $^{56}\text{Fe}(p,\gamma)$ reaction

a. *The 3774 keV resonance.* The angular distribution results in Table II allow only spin  $\frac{5}{2}$  assignment. The strong transition to the  $\frac{7}{2}^-$  g.s., together with the anisotropy of the angular distribution, rule out a spin  $\frac{1}{2}$  assignment. As this is a strong resonance an assignment of  $l_p=2$  seems more likely. Such an assignment is also supported by the small multipole mixing ratios measured for transitions from this resonance to the g.s., the 1378 and 1757 keV states of  $0.0\pm 0.01$ ,  $-0.035\pm 0.035$ , and  $-0.035\pm 0.035$ , respectively [see Figs. 6(a)–6(c) and Table II.] Using the Weisskopf estimates for single particle proton states, one expects a mixing ratio of 0.0046 for an  $E1/M2$  transition but 0.220 for an  $M1/E2$  transition. With any  $E2$  enhancement the latter value would be even larger and will be outside the experimental limits. Assuming  $E1/M2$  transitions from the  $E_p=3774$  keV resonance, the parity of this resonance is then positive. Thus the spin and parity of this resonance is taken to be  $\frac{5}{2}^+$ .

On the basis of the assignment  $J^\pi=\frac{5}{2}^+$  for the  $E_p=3774$  keV resonance, the  $\chi^2$  fits [Fig. 6(d)] for  $R\rightarrow 4675$  keV allow only a spin of  $\frac{5}{2}$  (with  $\delta=0.176\pm 0.035$ ) or  $\frac{7}{2}$  (with  $\delta=0.287\pm 0.021$ ) for the  $E_x=4675$  keV state. Based on the single-particle (Weisskopf estimate), a  $J^\pi=\frac{7}{2}^+$  assignment can be ruled out. Using similar arguments as above, the magnitude of the multipole mixing ratio for this transition is consistent with  $M1/E2$  character (see Table II). We therefore adopt an assignment of  $\frac{5}{2}^+$  for the state at  $E_x=4675$  keV.

b. *The 3794 keV resonance.* Based on the mode of decay, various spin values for this resonance were assumed. The  $\chi^2$  analysis of the primary transitions to the g.s. ( $\frac{7}{2}^-$ ) and 1897 keV ( $\frac{7}{2}^-$ ) states allows only a spin assignment of  $\frac{3}{2}$  or  $\frac{5}{2}$  for this resonant state at  $E_x=9754$  keV. The

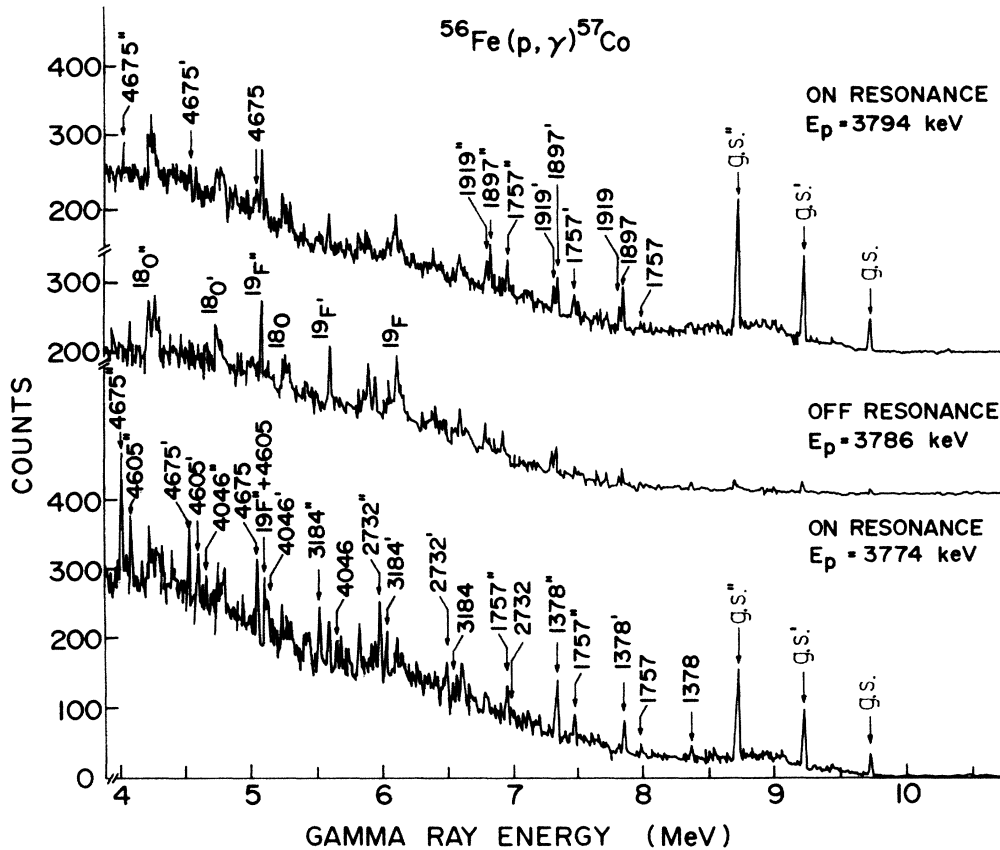


FIG. 2. Gamma-ray spectra from the  $^{56}\text{Fe}(p,\gamma)^{57}\text{Co}$  reaction taken at  $E_p=3774$  keV (on resonance),  $E_p=3786$  keV (off resonance), and  $E_p=3794$  keV (on resonance).

$\chi^2$  plots of the  $9754 \rightarrow \text{g.s.}$  and  $9754 \rightarrow 1897$  transitions are shown in Figs. 7(a) and 7(b), respectively. The  $J^\pi = \frac{3}{2}^\pm$  assignment can be ruled out when compared with the Weisskopf estimate for single-particle proton states (Table II). A  $J^\pi = \frac{5}{2}^-$  for this resonance is quite unlikely using similar arguments as above. It can be seen from Table II

that the  $d$ -wave nature of this resonance is supported by the small experimental  $\delta$  when compared with the Weisskopf estimate for both primary transitions. As a result, a  $J^\pi = \frac{5}{2}^+$  is assigned to this resonant state at  $E_x = 9754$  keV.

Using  $J = \frac{5}{2}$  for the  $E_p = 3794$  keV resonance, the  $\chi^2$  fits for the primary transitions to the state at 4675 keV [Fig. 7(c)] indicate that the spin of the 4675 keV state is either  $\frac{3}{2}$  or  $\frac{5}{2}$ . The magnitude of  $\delta$  for this transition is consistent with  $M1/E2$  character as indicated in Table II. As a result, a  $J^\pi = \frac{5}{2}^+$  is assigned to the state at  $E_x = 4675$  keV, which is consistent with the results obtained for the same level at the  $E_p = 3774$  keV resonance. This level was also observed by Rosner and Holbrow<sup>16</sup> at  $4689 \pm 20$  keV in the  $^{56}\text{Fe}(^3\text{He},d)^{57}\text{Co}$  reaction as a result of an  $l=2$  proton transfer.

## 2. Angular distribution of $\gamma$ rays from the $^{56}\text{Fe}(p,p'\gamma)$ reaction

In order to confirm the spins of the resonances, the angular distributions of the 845 keV  $\gamma$  ray were measured at the  $E_p = 3774$  and 3794 keV resonances. The advantage of the  $(p,p'\gamma)$  reaction lies in the fact that, following an inelastic scattering process, the  $\gamma$  decay of the excited states of a medium-heavy nucleus usually occurs with relatively low energy  $\gamma$  rays. These can easily be detected by Ge(Li)

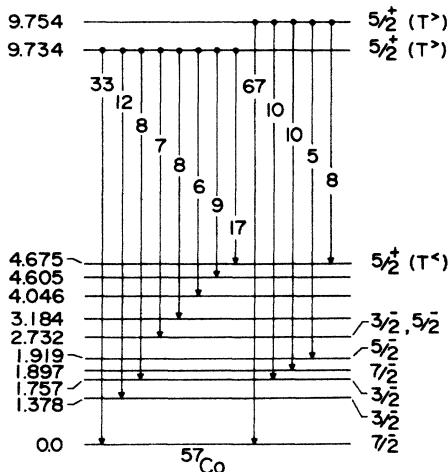


FIG. 3. Gamma decay scheme of the  $\frac{5}{2}^+$  IAS at  $E_p=3774$  and 3794 keV. The branching ratios are in percent. The energies at left are in MeV.

TABLE I. Summary of the Legendre polynomial coefficients.

Proton energy (keV)	Transition $E_i \rightarrow E_f$ (keV)	Legendre polynomial	
		$A_2/A_0$	$A_4/A_0$
3774	9734 $\rightarrow$ g.s.	$-0.141 \pm 0.06$	$-0.0156 \pm 0.080$
	9734 $\rightarrow$ 1378	$-0.329 \pm 0.11$	$-0.0505 \pm 0.149$
	9734 $\rightarrow$ 1757	$-0.315 \pm 0.20$	$0.0117 \pm 0.286$
	9734 $\rightarrow$ 4675	$0.248 \pm 0.07$	$-0.0638 \pm 0.095$
	845 $\rightarrow$ g.s. $^{56}\text{Fe}(p,p'\gamma)$	$0.401 \pm 0.03$	$-0.508 \pm 0.039$
3794	9754 $\rightarrow$ g.s.	$-0.127 \pm 0.04$	$0.010 \pm 0.046$
	9754 $\rightarrow$ 1897	$-0.318 \pm 0.09$	$0.006 \pm 0.127$
	9754 $\rightarrow$ 4675	$0.238 \pm 0.08$	$0.0399 \pm 0.111$
	845 $\rightarrow$ g.s. $^{56}\text{Fe}(p,p'\gamma)$	$0.369 \pm 0.01$	$-0.380 \pm 0.016$

detectors with excellent resolution and reasonable efficiency.

The angular distribution data for the  $\gamma$  quanta deexciting the 845 keV state in  $^{56}\text{Fe}$  at the proton energies  $E_p=3774$  and  $3794$  keV are shown in Figs. 4(e) and 5(d). Assuming a resonance spin and parity of  $\frac{5}{2}^+$  and pure

$s_{1/2}$  outgoing protons in the inelastic channel, the angular distribution of the  $E2$   $\gamma$  quanta should have the following coefficients:<sup>17</sup>  $A_2=0.57$  and  $A_4=-0.57$ . In the present measurements the normalized Legendre polynomial values for the 845 keV  $\gamma$  ray at the  $E_p=3774$  and  $3794$  keV resonances which resulted from fitting the experimental angular distribution data are  $A_2=0.401 \pm 0.03$ ,  $A_4=-0.508 \pm 0.039$  and  $A_2=0.369 \pm 0.01$ ,  $A_4=-0.380 \pm 0.016$ , respectively (see Table I). A comparison of the theoretical and experimental  $A_2$  and  $A_4$  coefficients provides further supporting evidence that both resonances are indeed  $\frac{5}{2}^+$  resonances.

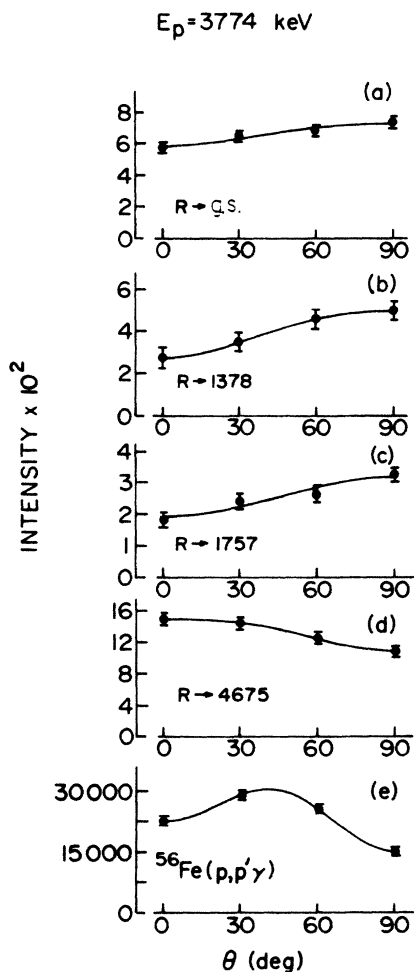


FIG. 4. Least-squares fit to the experimental angular distribution for  $\gamma$  rays at the  $E_p=3774$  keV resonance. R and g.s. represent the resonance and ground state, respectively.

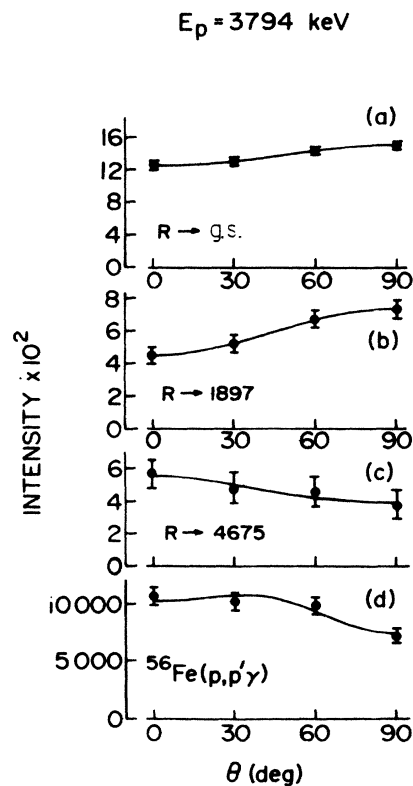


FIG. 5. Least-squares fits to the experimental angular distribution for  $\gamma$  rays at the  $E_p=3794$  keV resonance. R and g.s. represent the resonance and ground state, respectively.

## IV. DISCUSSION

## A. Analog state identification

As described in the preceding section, the resonances at  $E_p=3774$  and  $3794$  keV are unambiguously assigned to be of  $J^\pi=\frac{5}{2}^+$  character from  $(p,\gamma)$  and  $(p,p'\gamma)$  angular

distributions. The other two resonances at  $E_p=3816$  and  $3822$  keV are likely to be of  $J=\frac{3}{2}$  or  $\frac{5}{2}$  type. However, only the two  $J^\pi=\frac{5}{2}^+$  states have measurable gamma transition strengths. If we consider these two the  $d_{5/2}$  IAR fragments and use the relation  $\Delta E_C=E_p^{c.m.}$

TABLE II. Comparison of the mixing ratio  $\delta$  with the Weisskopf estimate for the studied resonant states of  $^{57}\text{Co}$ .

Resonance $E_p \pm 1$ (keV)	Transition $E_i \rightarrow E_f$ (keV)	Transition $J_i^\pi \rightarrow J_f^\pi$	Character	Weisskopf estimate for $ \delta $	Experimental mixing ratio $\delta$	Assigned $J^\pi$	
3774	9734 $\rightarrow$ g.s.	$\frac{3}{2}^- \rightarrow \frac{7}{2}^-$	$E2 (M3)$	0.0036	$-0.287 \pm 0.006$	$J_i^\pi = \frac{5}{2}^+$	
		$\frac{3}{2}^+ \rightarrow \frac{7}{2}^-$	$M2 (E3)$	0.179	$-0.287 \pm 0.006$		
		$\frac{5}{2}^- \rightarrow \frac{7}{2}^-$	$M1 (E2)$	0.220	$0.0 \pm 0.01$		
		$\frac{5}{2}^+ \rightarrow \frac{7}{2}^-$	$E1 (M2)$	0.0046	$0.0 \pm 0.01$		
	9734 $\rightarrow$ 1378	$\frac{3}{2}^- \rightarrow \frac{3}{2}^-$	$\frac{3}{2}^- \rightarrow \frac{3}{2}^-$	$M1 (E2)$	0.189	$0.53 \pm_{0.01}^{0.03}$	$J_i^\pi = \frac{5}{2}^+$
			$\frac{3}{2}^+ \rightarrow \frac{3}{2}^-$	$E1 (M2)$	0.0039	$0.53 \pm_{0.01}^{0.03}$	
			$\frac{5}{2}^- \rightarrow \frac{3}{2}^-$	$M1 (E2)$	0.189	$-0.035 \pm 0.035$	
			$\frac{5}{2}^+ \rightarrow \frac{3}{2}^-$	$E1 (M2)$	0.0039	$-0.035 \pm 0.035$	
	9734 $\rightarrow$ 1757	$\frac{3}{2}^- \rightarrow \frac{3}{2}^-$	$\frac{3}{2}^- \rightarrow \frac{3}{2}^-$	$M1 (E2)$	0.181	$0.532 \pm_{0.07}^{0.035}$	$J_i^\pi = \frac{5}{2}^+$
			$\frac{3}{2}^+ \rightarrow \frac{3}{2}^-$	$E1 (M2)$	0.0037	$0.532 \pm_{0.07}^{0.035}$	
			$\frac{5}{2}^- \rightarrow \frac{3}{2}^-$	$M1 (E2)$	0.181	$-0.035 \pm 0.035$	
			$\frac{5}{2}^+ \rightarrow \frac{3}{2}^-$	$E1 (M2)$	0.0037	$-0.035 \pm 0.035$	
9734 $\rightarrow$ 4675	$\frac{5}{2}^+ \rightarrow \frac{3}{2}^-$	$\frac{5}{2}^+ \rightarrow \frac{3}{2}^-$	$E1 (M2)$	0.0024	$-0.287 \pm 0.017$	$J_f^\pi = \frac{5}{2}^+$	
		$\frac{5}{2}^+ \rightarrow \frac{3}{2}^+$	$M1 (E2)$	0.115	$-0.287 \pm 0.017$		
		$\frac{5}{2}^+ \rightarrow \frac{5}{2}^-$	$E1 (M2)$	0.0024	$0.176 \pm 0.035$		
		$\frac{5}{2}^+ \rightarrow \frac{5}{2}^+$	$M1 (E2)$	0.115	$0.176 \pm 0.035$		
		$\frac{5}{2}^+ \rightarrow \frac{7}{2}^-$	$E1 (M2)$	0.0024	$0.287 \pm 0.021$		
		$\frac{5}{2}^+ \rightarrow \frac{7}{2}^+$	$M1 (E2)$	0.115	$0.287 \pm 0.021$		
3794	9754 $\rightarrow$ g.s.	$\frac{3}{2}^- \rightarrow \frac{7}{2}^-$	$E2 (M3)$	0.0036	$-0.249 \pm 0.017$	$J_i^\pi = \frac{5}{2}^+$	
		$\frac{3}{2}^+ \rightarrow \frac{7}{2}^-$	$M2 (E3)$	0.179	$-0.249 \pm 0.017$		
		$\frac{5}{2}^- \rightarrow \frac{7}{2}^-$	$M1 (E2)$	0.221	$0.0 \pm 0.03$		
		$\frac{5}{2}^+ \rightarrow \frac{7}{2}^-$	$E1 (M2)$	0.0046	$0.0 \pm 0.03$		
	9754 $\rightarrow$ 1897	$\frac{3}{2}^- \rightarrow \frac{7}{2}^-$	$\frac{3}{2}^- \rightarrow \frac{7}{2}^-$	$E2 (M3)$	0.0029	$-0.44 \pm 0.017$	$J_i^\pi = \frac{5}{2}^+$
			$\frac{3}{2}^+ \rightarrow \frac{7}{2}^-$	$M2 (E3)$	0.144	$-0.44 \pm 0.017$	
			$\frac{5}{2}^- \rightarrow \frac{7}{2}^-$	$M1 (E2)$	0.178	$-0.069 \pm 0.017$	
			$\frac{5}{2}^+ \rightarrow \frac{7}{2}^-$	$E1 (M2)$	0.0037	$-0.069 \pm 0.017$	
	9754 $\rightarrow$ 4675	$\frac{5}{2}^+ \rightarrow \frac{3}{2}^-$	$\frac{5}{2}^+ \rightarrow \frac{3}{2}^-$	$E1 (M2)$	0.0024	$-0.325 \pm 0.017$	$J_f^\pi = \frac{5}{2}^+$
			$\frac{5}{2}^+ \rightarrow \frac{3}{2}^+$	$M1 (E2)$	0.115	$-0.325 \pm 0.017$	
			$\frac{5}{2}^+ \rightarrow \frac{5}{2}^-$	$E1 (M2)$	0.0024	$0.176 \pm 0.035$	
			$\frac{5}{2}^+ \rightarrow \frac{5}{2}^+$	$M1 (E2)$	0.115	$0.176 \pm 0.035$	

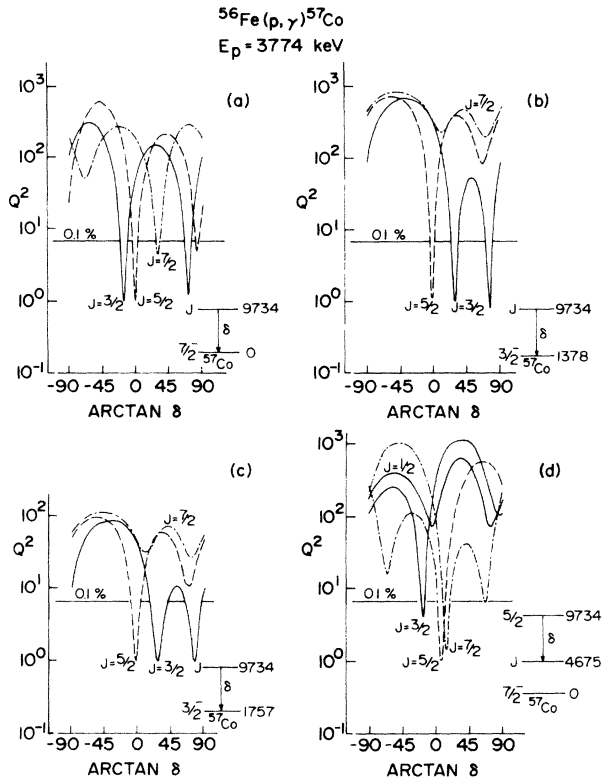


FIG. 6. Values of  $Q^2$  vs  $\arctan \delta$  from fitting experimental angular distribution to theory for different spin values at the  $E_p = 3774$  keV resonance.

$+B_n - E_x$ , where  $B_n$  is the binding energy of the last neutron in the parent nucleus (7642 keV for  $^{57}\text{Fe}$ ) and  $E_x = 2506$  keV is the excitation energy of the parent state, we obtain an average  $\Delta E_C = 8854$  keV as the Coulomb displacement energy. The corresponding value<sup>1</sup> for  $\frac{9}{2}^+$  IAR in  $^{57}\text{Co}$  is 8845 keV. Thus the consideration of spins, Coulomb displacement energies, and the  $\gamma$ -decay modes support the argument that the two  $J^\pi = \frac{5}{2}^+$  states are the split analog of the  $^{57}\text{Fe}$  2506 keV state. This seems reasonable since their separation in energy is less than the spreading width characteristic of analog resonances.<sup>18</sup>

Brandle *et al.*<sup>8</sup> measured the high resolution excitation function of the  $^{56}\text{Fe}(p, p)$  reaction in the energy range  $E_p = 3700$ – $4300$  keV. They reported seven  $\frac{1}{2}^+$  states while no  $\frac{5}{2}^+$  IAR was observed in this energy range. In a high resolution experiment using the  $(p, p)$ ,  $(p, p')$ , and  $(p, p'\gamma)$  reactions on  $^{56}\text{Fe}$ , Watson *et al.*<sup>9</sup> have surveyed the energy region  $E_p = 3.1$ – $4.0$  MeV and reported 142  $d_{5/2}$  resonances. However, based on the Coulomb displacement energy of  $\Delta E_C = 8834$  keV they identified the strong resonance at  $E_p = 3764$  keV as a candidate for the expected  $d_{5/2}$  IAR. In an earlier study by Watson<sup>19</sup> using the same reactions and technique as in Ref. 9, he assigned  $J^\pi = \frac{5}{2}^+$  for the resonances at  $E_p = 3766.2$ , 3786.3, and 3808.3 keV, and the  $E_p = 3766.2$  keV resonance was assigned as the IAR candidate. Considering the accuracy of the proton energy, these resonance energies are in agree-

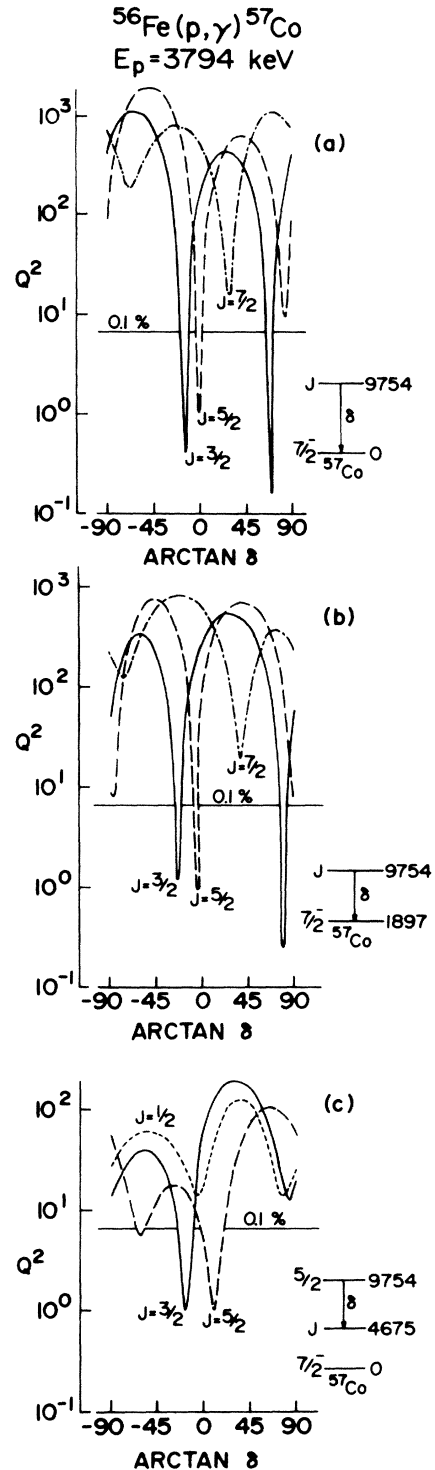


FIG. 7. Values of  $Q^2$  vs  $\arctan \delta$  from fitting experimental angular distribution to theory for different spin values at the  $E_p = 3794$  keV resonance.

ment with the  $E_p = 3774$ , 3794, and 3816 keV resonances reported in the present work. Our spin assignment of  $J^\pi = \frac{5}{2}^+$  for the first two resonances is in agreement with those given in Ref. 19. The remaining resonance at  $E_p = 3816$  keV is weak and obscured by interference with

neighboring levels; the gamma-decay properties and spin could not be determined accurately in the present work. Arai *et al.*<sup>10</sup> have independently performed another high resolution experiment using the  $^{56}\text{Fe}(p,p_0)$  reaction. They have reported 22  $d_{5/2}$  resonances in the  $E_p = 2.928\text{--}3.928$  MeV range. However, from the Coulomb energy systematics of other IAR's in this energy region, they identified the  $E_p = 3762.7$  keV resonance as the strongest  $d_{5/2}$  IAR fragment. In summary, our present results from  $(p,\gamma)$  and  $(p,p'\gamma)$  reactions supplement those reported earlier<sup>9,10,19</sup> from  $^{56}\text{Fe}(p,p)$ ,  $^{56}\text{Fe}(p,p_0)$ ,  $^{56}\text{Fe}(p,p')$ , and  $^{56}\text{Fe}(p,p'\gamma)$  reactions.

### B. Gamma decay properties of $d_{5/2}$ IAS's

The resonance strengths, defined as  $\omega_\gamma = (2J + 1)\Gamma_p\Gamma_\gamma/\Gamma$ , were extracted from  $\gamma$  spectra measured above and below the step in the thick target yield of  $\theta(p,\gamma) = 55^\circ$ . If it is assumed that  $\Gamma_p \geq \Gamma_\gamma$ , then the  $\gamma$ -ray width  $\Gamma_\gamma$  can be obtained from the resonance strength. In Table III the resonance strengths,  $\Gamma_\gamma$ , and partial widths,  $\Gamma_\gamma$ , of the primary  $\gamma$  transitions at the  $E_p = 3774$  and  $3794$  keV resonances are given. The strengths in single particle units and the reduced transition probabilities  $B(E1)$  and  $B(M1)$  in Table III are calculated with the assumed multipole orders of column 3.

From the present results, the level at  $E_x = 4675$  keV was not populated in the off resonance spectrum as shown in Fig. 2 and has been unambiguously assigned to be of  $J^\pi = \frac{3}{2}^+$  type from  $(p,\gamma)$  angular distributions at both IAR's. The  $E_x = 4675$  keV state is considered the  $T^<$  antianalog state, which can be identified with the one observed by Rosner and Holbrow<sup>16</sup> at  $4689 \pm 20$  keV from the  $^{56}\text{Fe}(^3\text{He,d})^{57}\text{Co}$  reaction as well as the level reported by Adams *et al.*<sup>20</sup> at  $4702$  keV and  $(2J + 1)S = 0.30$  from the  $^{56}\text{Fe}(d,n)^{57}\text{Co}$  reaction, as a result of an  $l = 2$  proton

transfer. From the spacing between the IAS and the  $4675$  keV state (AIAS), we obtain the symmetry potential value of  $V_1 = 114$  MeV. This is in good agreement with values for this parameter ( $V_1 \sim 100\text{--}150$  MeV) in this mass region.

If the IAS ( $T^>$ ) and AIAS ( $T^<$ ) are assumed to be the ones that a  $d_{5/2}$  particle weakly couples to an inert  $J = 0$ ,  $T = 2$  core, the calculated<sup>21</sup> isovectorial  $B(M1)$  single particle strength is  $B(M1) = 1.34$  W.u. The measured  $B(M1)$  strength, of  $3.27 \times 10^{-2}$  W.u., summed over the two  $d_{5/2}$  IAS fragments at  $E_p = 3774$  and  $3794$  keV is hindered by a factor of  $2.4 \times 10^{-2}$ , or  $2.4\%$  of the s.p. strength. This reduction in the IAS  $\rightarrow$  AIAS transition strength is attributed to the destructive interference between the single-particle and core-polarized transition amplitude. Such an explanation is supported by the fact that the  $d_{5/2}$  AIAS at  $4675$  keV has a low experimental spectroscopic factor.

### V. SUMMARY AND CONCLUSIONS

The  $d_{5/2}$  IAR's corresponding to the  $E_x = 2506$  keV,  $J^\pi = \frac{5}{2}^+$ ,  $S(d,p) = 0.122$  state<sup>22</sup> in  $^{57}\text{Fe}$  have been studied by the  $^{56}\text{Fe}(p,\gamma)^{57}\text{Co}$  and  $^{56}\text{Fe}(p,p'\gamma)$  reactions. Both IAS fragments at  $E_p = 3774$  and  $3794$  keV populated a state at  $E_x = 4675$  keV which has been identified as the AIAS. Gamma decay properties, in particular the branching ratios, resonance strengths, transition strengths, reduced transition probabilities  $B(E1)$  and  $B(M1)$ , and the  $\gamma$ -ray angular distributions from the capture and inelastic channels at both resonances, have been studied. We do not observe strong  $M1$  transitions to any of the low lying levels in  $^{57}\text{Co}$ . The reduction in the IAS  $\rightarrow$  AIAS  $B(M1)$  transition strength which amounts to  $2.4\%$  of the s.p. strength is explained qualitatively as a consequence of mixing core excitations into the wave function describing the antiana-

TABLE III.  $\gamma$ -decay properties of the  $d_{5/2}$  IAR fragments of the  $2506$  keV state in  $^{57}\text{Fe}$ .

Final state in $^{57}\text{Co}$	$J^\pi$	Multipole order	Resonance at $E_p = 3774$ keV			Resonance at $E_p = 3794$ keV			
			$\Gamma_\gamma$ (meV)	$ M ^2$ (W.u.) ( $\times 10^{-4}$ )	$B(M1)$ ( $\mu_N^2$ ) ( $\times 10^{-4}$ )	$B(E1)$ ( $e^2 \text{fm}^2$ ) ( $\times 10^{-4}$ )	$\Gamma_\gamma$ (meV)	$ M ^2$ (W.u.) ( $\times 10^{-4}$ )	$B(M1)$ ( $\mu_N^2$ ) ( $\times 10^{-4}$ )
0	$\frac{7}{2}^-$	E1	$88 \pm 10$	0.949	0.913	$366 \pm 47$	3.92		3.77
1378	$\frac{3}{2}^-$	E1	$32 \pm 4$	0.545	0.524				
1757	$\frac{3}{2}^-$	E1	$21 \pm 3$	0.419	0.403	$55 \pm 7$	1.07		1.03
1897	$\frac{7}{2}^-$	E1				$55 \pm 7$	1.13		1.09
1919	$\frac{5}{2}^-$	E1				$27 \pm 4$	0.558		0.536
2732	$\frac{3}{2}^-, \frac{5}{2}^-$	E1	$19 \pm 2$	0.541	0.521				
3184			$21 \pm 3$						
4046			$16 \pm 2$						
4605			$24 \pm 3$						
4675	$\frac{5}{2}^+$	M1	$46 \pm 6$	167	303	$44 \pm 6$	160	290	



log final state for the radiative transition.

In conclusion, we note that the  $M1$  strength in the  $d_{5/2}$  IAS  $\rightarrow$  AIAS transitions reaches a maximum in the middle of the  $f$ - $p$  shell and tends to fall off on either side. This feature could be interpreted as being due to increasing core-polarization effects as one departs from the closed  $f_{7/2}$  proton shell nuclei. The isovectorial  $M1$  strength distribution for  $d_{5/2}$  IAS's in the  $f$ - $p$  shell nuclei follows closely the same trend as the  $g_{9/2}$  IAS in this mass region. In order to make any quantitative comparison, full scale shell model calculations or the extension of existing theoretical models to treat core polarization simultaneously in more than one subshell and additional experimental data on similar transitions in neighboring nuclei would be extremely useful. Such data will help us

to understand better the structure of these nuclei in the  $f$ - $p$  shell.

#### ACKNOWLEDGMENTS

The authors acknowledge the hospitality and assistance of scientists at the Nuclear Research Center "Demokritos." In particular, thanks are due Professor G. Vourvopoulos for his interest and valuable discussions. We are also indebted to Professor P. W. Martin (University of British Columbia) for his invaluable discussions and critical reading of the manuscript. The work was supported by the University of Petroleum and Minerals and their financial support is gratefully acknowledged.

\*Author for correspondence. Present address: Department of Physics, University of British Columbia, Vancouver, British Columbia, Canada V6T 2A6.

†Present address: Department of Physics, Michigan State University, MI 48823.

<sup>1</sup>S. El-Kateb, M. Garwan, G. Vourvopoulos, and T. Paradellis, *J. Phys. G* **11**, 1179 (1985).

<sup>2</sup>M. Schrader, H. V. Klapdor, G. Bergdolt, and A. M. Bergdolt, *Phys. Lett.* **60B**, 39 (1975), and references therein.

<sup>3</sup>H. V. Klapdor, *Phys. Lett.* **35B**, 405 (1971).

<sup>4</sup>S. Maripuu, *Phys. Lett.* **31B**, 181 (1970).

<sup>5</sup>V. P. Alshein, *Izv. Akad. Nauk SSSR, Ser. Fiz.* **37**, 1959 (1973) [*Bull. Acad. Sci. USSR, Phys. Ser.* **37**, 137 (1973)].

<sup>6</sup>M. Didler Hossain, *Nuovo Cimento* **39A**, 594 (1977).

<sup>7</sup>C. Rangacharyulu, M. B. Chatterjee, C. Pruneau, and C. St-Pierre, *Can. J. Phys.* **60**, 815 (1982).

<sup>8</sup>H. Brändle, W. R. Wylie, F. Zamboni, and W. Zych, *Nucl. Phys.* **A151**, 211 (1970).

<sup>9</sup>W. A. Watson III, E. G. Bilpuch, and G. E. Mitchell, *Phys. Rev. C* **24**, 1992 (1981).

<sup>10</sup>E. Arai, M. Futakuchi, H. Kamada, J. Komaki, T. Matsuzaki, M. Ogawa, and Y. Oguri, *Nucl. Phys.* **A378**, 259 (1982).

<sup>11</sup>J. B. Marion and F. C. Young, *Nuclear Reaction Analysis* (North-Holland, Amsterdam, 1968).

<sup>12</sup>M. A. Meyer, N. S. Wolmarans, and D. Reitman, *Nucl. Phys.* **A144**, 261 (1970).

<sup>13</sup>R. J. De Meijer, H. S. Plendl, and R. Holub, *At. Data Nucl. Data Tables* **13**, 1 (1974).

<sup>14</sup>G. I. Harris, H. J. Hennecke, and D. D. Watson, *Phys. Rev. B* **139**, 1113 (1965).

<sup>15</sup>A. J. Ferguson, *Angular Correlation Methods in Gamma-Ray Spectroscopy* (North-Holland, Amsterdam, 1965).

<sup>16</sup>B. Rosner and C. H. Holbrow, *Phys. Rev.* **154**, 1080 (1967).

<sup>17</sup>E. Sheldon and D. M. Van Patter, *Rev. Mod. Phys.* **38**, 143 (1966).

<sup>18</sup>A. M. Lane and J. M. Soper, *Nucl. Phys.* **37**, 663 (1962).

<sup>19</sup>W. A. Watson, Ph.D. dissertation, Duke University, 1980 (unpublished).

<sup>20</sup>A. Adam, O. Bersillon, and S. Joly, *Phys. Rev. C* **14**, 92 (1976).

<sup>21</sup>R. D. Lawson, *Theory of the Nuclear Shell Model* (Clarendon, Oxford, 1980).

<sup>22</sup>R. L. Auble, *Nucl. Data Sheets* **20**, 327 (1977).